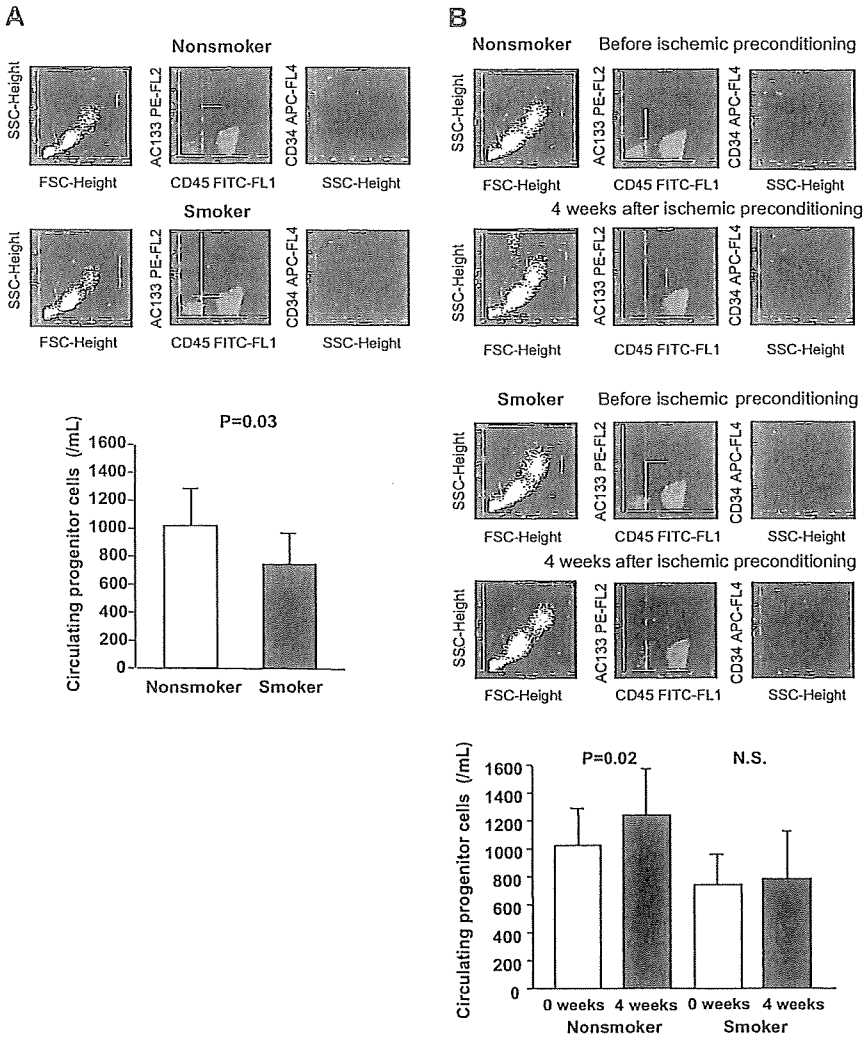


Figure 2. A, Measurement of the number of progenitor cells by flow cytometer before ischemic preconditioning in nonsmokers and smokers. B, Comparison of the number of circulating progenitor cells at 0 weeks and 4 weeks of ischemic preconditioning in nonsmokers and smokers.

to 32.4±6.6 mL/min per 100 mL of tissue ($P$=0.002) by 4 weeks of IPC in the nonsmoker group but was not altered in the 4-week follow-up period in the smoker group (Figure 1). The increases in FBF during infusion of SNP were similar at the beginning and the end of the 4-week study period in both the nonsmoker group and smoker group (Figure 1). No significant change was observed in arterial blood pressure or heart rate with intra-arterial infusion of ACh and SNP.

Intra-arterial infusion of L-NMMA significantly decreased baseline FBF from 4.9±0.4 to 4.2±0.3 mL/min per 100 mL of tissue ($P$<0.001) in the nonsmoker group and from 5.0±0.7 to 4.3±0.4 mL/min per 100 mL of tissue ($P$<0.001) in the smoker group before IPC stimulus and from 5.2±0.6 to 4.2±0.4 mL/min per 100 mL of tissue ($P$<0.001) in the nonsmoker group and from 4.9±0.6 to 4.1±0.3 mL/min per 100 mL of tissue ($P$<0.001) in the smoker group after IPC stimulus. Baseline FBF after L-NMMA infusion was similar in the 2 groups before (0 weeks) and after (4 weeks) the IPC stimulus. Intra-arterial infusion of L-NMMA decreased the response to ACh in the nonsmokers and smokers before and after the IPC stimulus ($P$<0.001, respectively; Figure 1). After L-NMMA infusion, FBF responses to ACh were similar in the 2 groups at 0 weeks and 4 weeks ($P$<0.001, respectively; Figure 1). Intra-arterial infusion of L-NMMA decreased the response to ACh before and after the IPC stimulus in the nonsmokers and smokers (Figure 1). After L-NMMA infusion, FBF responses to ACh were similar at 0 weeks and 4 weeks in the 2 groups (Figure 1). Neither arterial blood pressure nor heart rate was significantly changed by intra-arterial infusion of ACh in the presence of L-NMMA.

## Effects of IPC on Circulating Progenitor Cells

The number of circulating progenitor cells was significantly less in smokers than in nonsmokers before and after IPC (Figure 2A and 2B). IPC stimulus for 4 weeks increased the number of circulating progenitor cells from 1029±261 to 1232±341 mL ($P$=0.02) in nonsmokers, whereas there was no significant difference between the number of circulating progenitor cells at 0 weeks and that at 4 weeks in smokers (Figure 2B). Cells demonstrating double-positive staining lectin and 3,3,3′,3′-tetramethylindo-carbocyanine perchlorate-labeled acetylated low-density lipoprotein (Dil-AcLDL) were identified to be progenitor cells (Figure 3A). Cell migration response to VEGF was significantly less in smokers than in nonsmokers before and after IPC (Figure 3B and 3C). IPC stimulus for 4 weeks increased cell migration response to

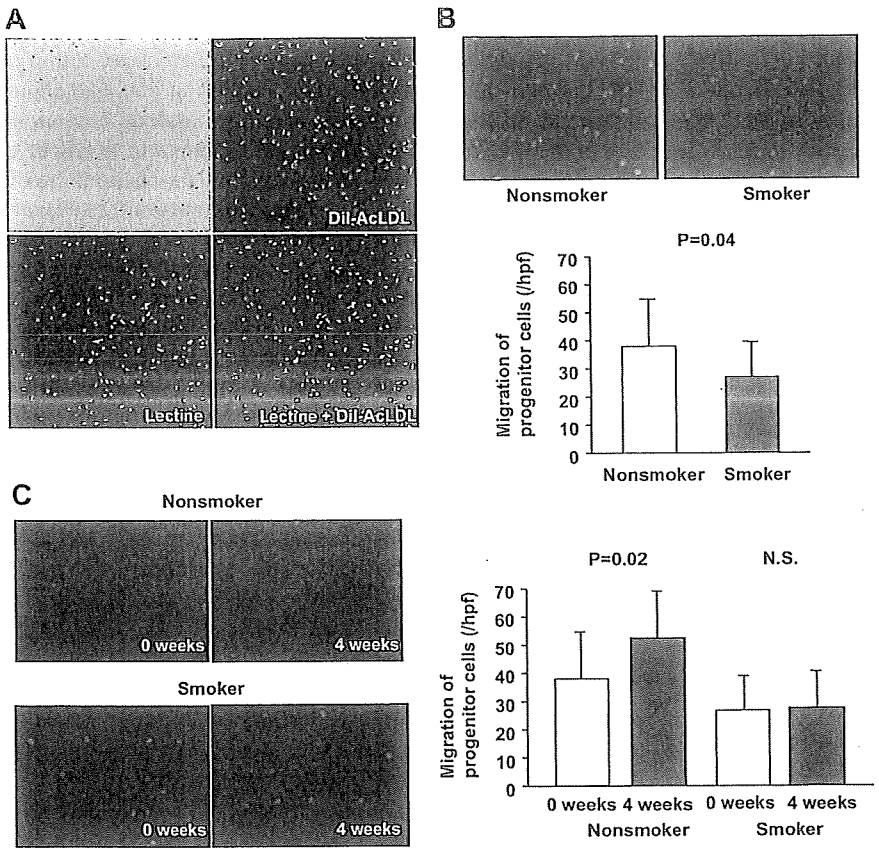


**Figure 3.** A, Characterization of progenitor cells by immunofluoresence for lectin binding (green), DiI-AcLDL uptake (red) and lectin/DiI-AcLDL double-positive cells (yellow; ×100). B, Measurement of the migration of cells labeled with 4′,6-diamidino-2-phenylindole by fluorescence before ischemic preconditioning in nonsmokers and smokers (×200). C, Measurement of the migration of cells labeled with 4′,6-diamidino-2-phenylindole by fluorescence at 0 weeks and 4 weeks of ischemic preconditioning in nonsmokers and smokers (left; ×200). Comparison of the migration of progenitor cells in nonsmokers and that in smokers at 0 weeks and 4 weeks of ischemic preconditioning (right).

VEGF from 38±16 to 52±17 per high-power field ($P$=0.02) in nonsmokers, whereas there was no significant difference between cell migration response to VEGF at 0 weeks and that at 4 weeks in smokers (Figure 3C).

Changes in maximal FBF response to ACh correlated with changes in the number of circulating progenitor cells ($r$=0.59; $P$=0.002) and changes in cell migration response to VEGF ($r$=0.36; $P$=0.04) in the nonsmoker group (Figure 4) but not in the smoker group. There was a significant relationship between changes in the number of circulating progenitor cells and changes in cell migration response to VEGF ($r$=0.49; $P$=0.01) in the nonsmoker group (Figure 4) but not in the smoker group. There were no correlations between changes in the number of circulating progenitor cells and migration of progenitor cells and increase in plasma VEGF concentration. No correlation was found between changes in maximal FBF response to ACh and changes in blood pressure, heart rate, VEGF, or other variables or between these variables and changes in maximal FBF response to SNP in the 2 groups.

## Discussion

Four weeks of repetition of IPC stimulus augmented FBF response to ACh but not FBF response to SNP in nonsmokers, whereas repetition of IPC stimulus did not alter either FBF response to ACh or that to SNP in smokers. L-NMMA abolished the IPC stimulus-induced augmentation of endothelium-dependent vasodilation in nonsmokers. In addition, the increases in maximal FBF response to ACh correlated with the increases in the number of circulating progenitor

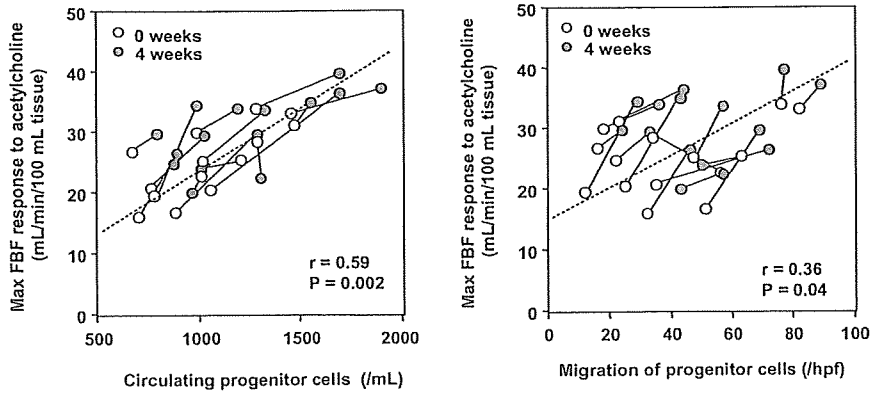


**Figure 4.** Correlations between maximal FBF response to ACh and number of circulating progenitor cells (left) and migration of progenitor cells (right) at 0 weeks and 4 weeks of ischemic preconditioning in nonsmokers.

cells and migration of progenitor cells after repetition of IPC. These findings suggest that the augmentation of ACh-induced vasodilation may be related to an improvement in the function of the endothelium, not that of vascular smooth muscle, and may be because of an increase in NO production through, at least in part, an increase in circulating progenitor cells.

In the present study, to evaluate the role of smoking, per se, in IPC stimulus-induced changes in endothelial function, we selected healthy young men to avoid the possibility of alteration in endothelial function and number of circulating progenitor cells and function of progenitor cells caused by factors such as hypertension, heart failure, atherosclerosis, hypercholesterolemia, diabetes mellitus, aging, and menstrual cycle.

There are several possible explanations for the IPC stimulus-induced augmentation of endothelium-dependent vasodilation in humans. Several lines of evidence have shown that the "late" effect of IPC is mainly attributed to an increase in NO production.[4,5,21,22] In the present study, L-NMMA completely abolished the IPC stimulus-induced augmentation of FBF responses to ACh. In a recent study, the nonselective NO synthase inhibitor $N^{\omega}$-nitro-L-arginine, but not the inducible NO synthase inhibitor 1400W, completely eliminated the protective effects of IPC against coronary endothelial injury.[21] Bolli et al[22] proposed that NO plays a prominent role in initiating IPC. These findings suggest that the beneficial effects of IPC repetition are attributed to activation of endothelial NO synthase, resulting in increased NO production.

Several lines of evidence have indicated that hypoxia, per se, enhances VEGF gene expression.[23,24] It is well known that VEGF gene expression is upregulated by HIF-1 under the condition of hypoxia.[24] HIF-1 is a heterodimer composed of 2 subunits, HIF-1$\alpha$ and HIF-1$\beta$, and promotes transcription by combining with hypoxia response element in its target gene.[24] In the present study, repetition of IPC increased plasma VEGF levels. Increases in maximal FBF response to ACh correlated with changes in the number of circulating progenitor cells and cell migration response to VEGF after repetition of IPC. Recently, Hill et al[14] also found by measurements of flow-mediated vasodilation in healthy men that the number of circulating progenitor cells is correlated with endothelial function. It has been shown that VEGF-induced and ischemia-induced mobilization of bone marrow-derived EPCs contribute to neovascularization.[25] Increases in VEGF gene expression and circulating VEGF levels with repetition of IPC may increase the levels of circulating progenitor cells and lead to an increase in capillary density, resulting in augmentation of endothelial function through an increase in NO production. Wang et al[6] reported significant increases in the number of functional capillaries and arteriole diameter in rats 24 hours after ischemic reperfusion. These findings suggest that the hypoxia-HIF-1-VEGF pathway may play an important role in IPC-induced angiogenesis in skeletal muscle. We showed a putative model of VEGF-modulating endothelial NO synthase activation by repetition of IPC (please see the online Data Supplement for additional details, Figure S2).

Although the precise mechanisms by which repetition of IPC stimulus does not induce augmentation of endothelium-dependent vasodilation in smokers remain unclear, inactivation of the VEGF-EPC pathway may contribute to failure of IPC-induced augmentation of endothelial function. In the present study, the number of circulating progenitor cells was decreased, and progenitor cell function was impaired in smokers compared with that of nonsmokers. These findings are consistent with results of previous studies.[26,27] In addition, although plasma concentration of VEGF increased after 4 weeks of IPC in smokers, as well as in nonsmokers, increases in VEGF levels did not increase the number of circulating progenitor cells and did not enhance the function of progenitor cells in smokers, whereas IPC stimuli increased the number of circulating progenitor cells and enhanced the function of progenitor cells in nonsmokers. Recently, Edirisinghe et al[28] have shown a potential mechanism for smoking-induced endothelial dysfunction. In mouse lung and human endothelial cells in vitro, cigarette smoking downregulated VEGF receptor-2 expression, endothelial NO synthase protein levels, and VEGF-induced VEGF receptor-2 phosphorylation, leading to impaired VEGF-induced cell migration and angiogenesis. It has been suggested that systemic inflammation and oxidative stress influence the number of circulating progenitor cells and function of progenitor cells.

In the present study, urinary excretion of 8-OHdG, an oxidative stress marker, was significantly higher in smokers than in nonsmokers and was correlated with maximal FBF response to ACh. Under the condition of excess oxidative stress, depletion of VEGF-induced mobilization of progenitor cells and enhancement of progenitor cell function and inactivation of NO bioavailability may form a vicious circle, leading to a lack of IPC-induced augmentation of endothelial function in smokers.

Several lines of evidence have shown that cigarette smoking is associated with systemic inflammation.[29–31] In the present study, levels of inflammation markers, interleukin 6, and hs-CRP were also significantly higher in smokers than in nonsmokers. Inflammation has a dual-sword role in EPC function. Although a low grade of inflammation, which probably has a favorable effect on EPCs, augments EPC functions, such as mobilization, proliferation, and colony formation, a high grade of inflammation inhibits EPC functions.[32,33] Interestingly, Verma et al[34] have reported that C-reactive protein, per se, directly inhibits EPC differentiation, survival, and function. Inflammation-induced impairment of EPC function might lead to a lack of IPC-induced augmentation of endothelial function in smokers. Clinical studies have shown that there is an association between inflammation and endothelial dysfunction.[35,36] In the present study, there was no association between vascular response to ACh and levels of inflammation markers interleukin 6 and hs-CRP, suggesting that systemic inflammation might not directly affect endothelial function in smokers. In addition, both interleukin 6 and hs-CRP were unchanged after the repetition of IPC stimulus in both groups.

## Study Limitations

In the present study, we examined the effect of IPC on vascular endothelial function in the absence of a prolonged

ischemia-reperfusion stimulus. Kharbanda et al[37] have shown that a clinically relevant period of ischemia reperfusion induces endothelial dysfunction in healthy subjects and that IPC attenuates endothelial dysfunction caused by ischemia reperfusion. It remains possible that IPC will prevent the attenuation of endothelium-dependent vasodilatation observed with an episode of ischemia-reperfusion injury in smokers without apparently altering the "basal state."

The present study is essentially a prospective single-arm study of IPC in 2 groups of subjects. A blinded, randomized, and crossover study design would enable a more specific conclusion concerning the role of smoking in IPC to be drawn.

Infusion of L-NMMA reduces basal endothelial NO release and FBF, confounding the interpretation of the inhibition of subsequent vasodilator responses. Coinfusion of L-NMMA with SNP to restore a steady-state NO would have improved the study design.

### Perspectives

Repetition of IPC augmented endothelial function through an increase in NO production. Endothelial dysfunction is the initial step in the pathogenesis of atherosclerosis, resulting in cardiovascular complications. It is important to select an appropriate intervention that is effective in improving or augmenting endothelial function. Repetition of IPC may be a simple, safe, and feasible therapeutic technique for endothelial protection of peripheral vessels. Furthermore, this technique has the potential to improve endothelial function as a new treatment for cardiovascular disease associated with endothelial dysfunction. Unfortunately, IPC might not have beneficial effects in smokers. Thus, nonsmoking and smoking cessation are important to prevent myocardial damage after severe ischemia, especially in patients with angina pectoris who have brief ischemic periods. Additional studies are needed to confirm the effects of IPC in the coronary artery in smokers.

## Acknowledgments

We thank Megumi Wakisaka and Satoko Michiyama for their excellent secretarial assistance.

## Sources of Funding

This study was supported in part by Grants-in-Aid for Scientific Research from the Ministry of Education, Science, and Culture of Japan (1559075100 and 1859081500).

## Disclosures

None.

## References

1. Ishihara M, Sato H, Tateishi H, Kawagoe T, Shimatani Y, Kurisu S, Sakai K, Ueda K. Implications of prodromal angina pectoris in anterior wall acute myocardial infarction. *J Am Coll Cardiol.* 1997;30:970–975.
2. Ishihara M, Inoue I, Kawagoe T, Shimatani Y, Kurisu S, Nishioka K, Kouno Y, Umemura T, Nakamura S, Sato H. Diabetes mellitus prevents ischemic preconditioning in patients with a first acute anterior myocardial infarction. *J Am Coll Cardiol.* 2001;38:1007–1011.
3. Murry CE, Jenninis RB, Reimer KA. Preconditioning with ischemia: a delay of lethal cell injury in ischemic myocardium. *Circulation.* 1986; 74:1124–1136.
4. Nakano A, Cohen MV, Downey JM. Ischemic preconditioning from basic mechanism to clinical applications. *Pharmacol Ther.* 2000;86: 263–275.
5. Laude K, Beauchamp P, Thuillez C, Richard V. Endothelial protective effects of preconditioning. *Cardiovasc Res.* 2002;55:466–473.
6. Wang WZ, Guo SZ, Anderson GL, Miller FN. The initiating factors of late preconditioning in skeletal muscle. *J Surg Res.* 2001;99:92–99.
7. Bolli R. The late phase of preconditioning. *Circ Res.* 2000;87:972–983.
8. Kloner RA, Lennings RB. Consequences of brief ischemia: stunning, preconditioning and their clinical implications part1. *Circulation.* 2001; 104:2981–2989.
9. Panza JA, Quyyumi AA, Brush JE Jr, Epstein SE. Abnormal endothelium-dependent vascular relaxation in patients with essential hypertension. *N Engl J Med.* 1990;323:22–27.
10. Drexler H, Horning B. Endothelial dysfunction in human disease. *J Mol Cell Cardiol.* 1999;31:51–60.
11. Higashi Y, Sasaki S, Kurisu S, Yoshimizu A, Ssaki N, Matsuura H, Kajiyama G, Oshima T. Regular aerobic exercise augments endothelium-dependent vascular relaxation in normotensive as well as hypertensive subjects: role of endothelium-derived nitric oxide. *Circulation.* 1999;100: 1194–1202.
12. Higashi Y, Sasaki S, Nakagawa K, Matsuura H, Oshima T, Chayama K. Endothelial function and oxidative stress in renovascular hypertension. *N Engl J Med.* 2002;346:1954–1962.
13. Kubo SH, Rector TS, Bank AJ, Williams RE, Heifetz SM. Endothelium-dependent vasodilation is attenuated in patients with heart failure. *Circulation.* 1991;84:1589–1596.
14. Hill JM, Zalos G, Halcox JP, Schenke WH, Waclawiw MA, Quyyumi AA, Finkel T. Circulating endothelial progenitor cells, vascular function, and cardiovascular risk. *N Engl J Med.* 2003;348:593–600.
15. Kimura M, Goto C, Umemura T, Ueda K, Nishioka K, Jitsuiki D, Yoshizumi M, Chayama K, Higashi Y. Repetition of ischemic preconditioning augments endothelium-dependent vasodilation in humans: role of endothelium-derived nitric oxide and endothelial progenitor cells. *Arterioscler Thromb Vasc Biol.* 2007;27:1403–1410.
16. Celermajer DS, Sorensen KE, Georgakopoulos D, Bull C, Thomas O, Robinson J, Deanfield JE. Cigarette smoking is associated with dose-related and potentially reversible impairment of endothelium-dependent dilation in healthy young adults. *Circulation.* 1993;88:2149–2155.
17. Lavi S, Prasad A, Yang EH, Mathew V, Simari RD, Rihal CS, Lerman LO, Lerman A. Smoking is associated with epicardial coronary endothelial dysfunction and elevated white blood cell count in patients with chest pain and early coronary artery disease. *Circulation.* 2007;115:2621–2627.
18. Barbash GI, White HD, Modan M, Diaz R, Hampton JR, Heikkila J, Kristinsson A, Moulopoulos S, Paolasso EA, Pehrsson K, Sandoe E, Simes J, Wilcox RG, Verstraete M, von der Lippe G, Van der Werf T. Significance of smoking in patients receiving thrombolytic therapy for acute myocardial infarction. Experience gleaned from the International Tissue Plasminogen Activator/Streptokinase Mortality Trial. *Circulation.* 1993;87:53–58.
19. Mueller HS, Cohen LS, Braunwald E, Forman S, Feit F, Ross A, Schweiger M, Cabin H, Davison R, Miller D, Solomon R, Knatterud GL, for the TIMI investigators. Predictors of early morbidity and mortality after thrombolytic therapy of acute myocardial infarction. Analyses of patient subgroups in the Thrombolysis in Myocardial Infarction (TIMI) Trial, phase II. *Circulation.* 1992;85:1254–1264.
20. Dimmeler S, Dernbach E, Zeiher AM. Phosphorylation of the endothelial nitric oxide synthase at ser-1177 is required for VEGF-induced endothelial cell migration. *FEBS Lett.* 2000;477:258–262.
21. Laude K, Richard V, Henry JP, Lallemand F, Thuillez C. Evidence against a role of inducible nitric oxide synthase in the endothelial protective effects of delayed preconditioning. *Brit J Pharmacol.* 2000;130: 1547–1552.
22. Bolli R, Dawn B, Tang XL, Qiu Y, Ping P, Xuan YT, Jones WK, Takano H, Guo Y, Zhang J. The nitric oxide hypothesis of late preconditioning. *Basic Res Cardiol.* 1998;93:325–338.
23. Olfert IM, Breen EC, Mathieu-Costello O, Wagner PD. Skeletal muscle capillarity and angiogenic mRNA levels after exercise training in normoxia and chronic hypoxia. *J Appl Physiol.* 2001;91:1176–1184.
24. Gustafsson T, Kraus WE. Exercise-induced angiogenesis-related growth and transcription factors in skeletal muscle, and their modification in muscle pathology. *Front Biosci.* 2001;6:D75–D89.
25. Asahara T, Takahashi T, Masuda H, Kalka C, Chen D, Iwaguro H, Inai Y, Silver M, Isner JM. VEGF contributes to postnatal neovascularization by

mobilizing bone marrow-derived endothelial progenitor cells. *EMBO J.* 1999;18:3964–3972.
26. Vasa M, Fichtlscherer S, Aicher A, Adler K, Urbich C, Martin H, Zeiher AM, Dimmeler S. Number and migratory activity of circulating endothelial progenitor cells inversely correlate with risk factors for coronary artery disease. *Circ Res.* 2001;89:E1–E7.
27. Kondo T, Hayashi M, Takeshita K, Numaguchi Y, Kobayashi K, Iino S, Inden Y, Murohara T. Smoking cessation rapidly increases circulating progenitor cells in peripheral blood in chronic smokers. *Arterioscler Thromb Vasc Biol.* 2004;24:1442–1447.
28. Edirisinghe I, Yang SR, Yao H, Rajendrasozhan S, Caito S, Adenuga D, Wong C, Rahman A, Phipps RP, Jin ZG, Rahman I. VEGFR-2 inhibition augments cigarette smoke-induced oxidative stress and inflammatory responses leading to endothelial dysfunction. *FASEB J.* 2008;22: 2297–2310.
29. Yanbaeva DG, Dentener MA, Creutzberg EC, Wesseling G, Wouters EF. Systemic effects of smoking. *Chest.* 2007;131:1557–1566.
30. Gill M, Dias S, Hattori K, Rivera ML, Hicklin D, Witte L, Girardi L, Yurt R, Himel H, Rafii S. Vascular trauma induces rapid but transient mobilization of VEGFR2(+)AC133(+) endothelial precursor cells. *Circ Res.* 2001;88: 167–174.
31. Seeger FH, Haendeler J, Walter DH, Rochwalsky U, Reinhold J, Urbich C, Rössig L, Corbaz A, Chvatchko Y, Zeiher AM, Dimmeler S. p38 mitogen-activated protein kinase downregulates endothelial progenitor cells. *Circulation.* 2005;111:1184–1191.
32. Güven H, Shepherd RM, Bach RG, Capoccia BJ, Link DC. The number of endothelial progenitor cell colonies in the blood is increased in patients with angiographically significant coronary artery disease. *J Am Coll Cardiol.* 2006;48:1579–1587.
33. Wu Y, Ip JE, Huang J, Zhang L, Matsushita K, Liew CC, Pratt RE, Dzau VJ. Essential role of ICAM-1/CD18 in mediating EPC recruitment, angiogenesis, and repair to the infarcted myocardium. *Circ Res.* 2006;99: 315–322.
34. Verma S, Kuliszewski MA, Li SH, Szmitko PE, Zucco L, Wang CH, Badiwala MV, Mickle DA, Weisel RD, Fedak PW, Stewart DJ, Kutryk MJ. C-reactive protein attenuates endothelial progenitor cell survival, differentiation, and function: further evidence of a mechanistic link between C-reactive protein and cardiovascular disease. *Circulation.* 2004; 109:2058–2067.
35. Oshima T, Ozono R, Yano Y, Oishi Y, Teragawa H, Higashi Y, Yoshizumi M, Kambe M. Association of helicobacter pylori infection with systemic inflammation and endothelial dysfunction in healthy male subjects. *J Am Coll Cardiol.* 2005;45:1219–1222.
36. Tonetti MS, D'Aiuto F, Nibali L, Donald A, Storry C, Parkar M, Suvan J, Hingorani AD, Vallance P, Deanfield J. Treatment of periodontitis and endothelial function. *N Engl J Med.* 2007;356:911–920.
37. Kharbanda RK, Peters M, Walton B, Kattenhorn M, Mullen M, Klein N, Vallance P, Deanfield J, MacAllister R. Ischemic preconditioning prevents endothelial injury and systemic neutrophil activation during ischemia-reperfusion in humans in vivo. *Circulation.* 2001;103: 1624–1630.

Hypertension Research (2010) 0, 1–6

www.nature.com/hr

ORIGINAL ARTICLE

# Increased leukocyte rho kinase (ROCK) activity and endothelial dysfunction in cigarette smokers

Takayuki Hidaka[1], Takaki Hata[1], Junko Soga[1], Yuichi Fujii[1], Naomi Idei[1], Noritaka Fujimura[1], Yasuki Kihara[1], Kensuke Noma[2], James K Liao[3] and Yukihito Higashi[2]

Rho-associated kinases (ROCKs) have been shown to be involved in the pathogenesis of atherosclerosis. Although smoking is associated with endothelial dysfunction and ROCK inhibitors improve endothelial function in smokers, it is not known whether ROCK activity is increased in smokers and whether this correlates with endothelial dysfunction. The purpose of this study was to evaluate the relationship between ROCK activity and endothelial function in smokers. We evaluated flow-mediated vasodilatation (FMD) using ultrasonography and ROCK activity in peripheral leukocytes using western blot analysis in 14 male smokers (28.1 ± 3.9 years) and 15 healthy male non-smokers (28.3 ± 3.6 years). ROCK activity was defined as the ratio of phospho-myosin-binding subunit (MBS) on myosin light-chain phosphatase to total MBS. FMD was significantly less in smokers than in non-smokers (4.7 ± 3.1 *vs.* 9.0 ± 3.8%, $P$=0.005). Nitroglycerine-induced vasodilation was similar in the two groups. ROCK activity was greater in smokers than in non-smokers (0.78 ± 0.27 *vs.* 0.54 ± 018, $P$=0.012). The expression of total MBS, ROCK1 and ROCK2 were similar in the two groups. ROCK activity correlated with systolic blood pressure ($r$=0.42, $P$=0.039). Multiple regression analysis revealed that smoking is an independent predictor of ROCK activity. There was a significant correlation between FMD and ROCK activity ($r$=−0.42, $P$=0.035). No other variable was correlated with FMD. These findings suggest that ROCK activity is enhanced by smoking and is a predictor of endothelial function.
*Hypertension Research* (2010) 0, 000–000. doi:10.1038/hr.2010.3

**Keywords:** endothelial function; Rho-associated kinase; smoker

## INTRODUCTION

Cigarette smoking is a major risk factor in the development of atherosclerosis[1,2] and independently increases clinical cardiovascular morbidity and mortality.[3] Several lines of evidence have shown that cigarette smoking alters hemostasis, causes inflammation and oxidative stress in vascular walls[4] and impairs endothelial function.[3,5] In addition, some studies have shown that cigarette smoking increases the numbers of circulating leukocytes and inflammatory markers such as C-reactive protein (CRP), interleukin-6 and soluble intercellular adhesion molecule type 1.[6,7]

Small guanosine triphosphate-binding protein RhoA (ras homolog gene family, member A) mediates various cellular physiologic functions such as cell proliferation, migration, adhesion, apoptosis and contraction,[8–11] all of which may be involved in the pathogenesis of atherosclerosis. Rho-associated kinases (ROCKs), which consist of two isoforms, ROCK1 and ROCK2, were found to be the immediate downstream targets of RhoA,[12] The RhoA/ROCK pathway has been shown to be involved in atherosclerotic lesion formation,[13] vasoconstriction[9,14] and myocardial hypertrophy[15] and to be activated in patients with hypertension[16] and coronary artery disease.[11,17] Previous studies using ROCK inhibitors such as fasudil or Y-27632 have suggested that ROCK may have an important role in the pathogenesis of cardiovascular disease.[9,13,15]

The vascular endothelium is involved in the release of various vasodilators, including nitric oxide (NO), prostaglandins and endothelium-derived hyperpolarizing factor as well as vasoconstrictors.[18] NO has an important role in the regulation of vascular tone, inhibition of platelet aggregation and suppression of smooth muscle cell proliferation.[19] Endothelial dysfunction is the initial step in the pathogenesis of atherosclerosis, resulting in cardiovascular and cerebrovascular outcomes. Previous studies have shown that activation of the RhoA/ROCK pathway impaired NO bioavailability through inhibition of endothelial NO synthase (eNOS) mRNA stability and eNOS protein phosphorylation at Ser 1177 through the Akt/ phosphoinositide 3-kinase pathway.[20]

Recently, it has been reported that ROCK activity is increased in subjects with metabolic syndrome and in patients with coronary artery disease.[11,21] In those studies, ROCK activity in peripheral leukocytes was directly assayed by western blot analysis using a specific antibody to phospho-myosin-binding subunit (MBS) on

[1]Department of Cardiovascular Medicine, Hiroshima University Graduate School of Biomedical Sciences, Hiroshima, Japan; [2]Department of Cardiovascular Physiology and Medicine, Hiroshima University Graduate School of Biomedical Sciences, Hiroshima, Japan and [3]Vascular Medicine Research Unit, Brigham and Women's Hospital and Harvard Medical School, Boston, MA, USA
Correspondence: Dr Y Higashi, Department of Cardiovascular Physiology and Medicine, Graduate School of Biomedical Sciences, Hiroshima University, 1-2-3 Kasumi, Mimami-ku, Hiroshima 734-8551, Japan.
E-mail: yhigashi@hiroshima-u.ac.jp
Received 15 October 2009; revised 27 November 2009; accepted 20 December 2009

myosin light-chain phosphatase, which is a downstream target of ROCK. As assessment of ROCK activity in peripheral leukocytes is minimally invasive and does not require pharmacologic intervention using intra-arterial infusion of ROCK inhibitors, it may be useful for evaluating ROCK activity in a clinical setting. Indeed, leukocyte ROCK activity has been shown to correlate inversely with endothelial function.[11]

We previously reported that intra-arterial infusion of the ROCK inhibitor, fasudil, improves endothelial function in smokers.[22] However, it is not known from these studies whether ROCK activity was higher in smokers and whether it correlated with endothelial dysfunction. The purpose of this study, therefore, is to determine whether ROCK activity is increased in smokers and whether this correlates with endothelial function.

## METHODS

### Subjects

We studied 14 male smokers (mean age: 28.1 ± 3.9 years) and 15 healthy male non-smokers (mean age: 28.3 ± 3.6 years) who had no history of cardiovascular disease, hypertension or other diseases. Normal blood pressure was defined as systolic blood pressure of <130 mm Hg and diastolic blood pressure of <80 mm Hg. The results of physical and routine laboratory examinations of the subjects were normal. None of the subjects were taking oral antioxidant vitamins or vasoactive drugs. Current smokers were defined as smokers who had smoked at least 1 pack-year, with 1 pack-year being defined as 20 cigarettes per day for 1 year. All of the smokers (19.1 ± 9.2 pack-years) had a current smoking history of more than 5 years and abstained from smoking for at least 3 h before the measurement of vascular function. We defined non-smokers as subjects who had never smoked. The study protocol was approved by the ethics committee of Hiroshima University Graduate School of Biomedical Sciences. Informed consent for participation in the study was obtained from all subjects.

### Measurement of FMD

All studies were performed in the morning, after overnight fasting, in a quiet, dark and air-conditioned room (constant temperature of 22–25 °C). The subjects remained supine throughout the study.

The vascular response to reactive hyperemia in the brachial artery was assessed for ultrasound assessment of endothelium-dependent flow-mediated vasodilatation (FMD). A high-resolution linear artery transducer (13 MHz) was coupled to computer-assisted analysis software (e-TRACKING system, Aloka, Tokyo, Japan) that used an automated edge detection system for measurement of brachial artery diameter. The subjects rested and the right arm was fixed by a special arm-holding device (MIST-100, Saraya, Osaka, Japan). A blood pressure cuff was placed around the forearm. The brachial artery was scanned longitudinally 5–10 cm above the elbow. When the clearest B-mode image of the anterior and posterior intimal interfaces between the lumen and vessel wall was obtained, the transducer was held at the same point throughout the scan by a special probe holder (MP-PH0001, ALOKA) to ensure consistency of the image. Depth and gain setting were set to optimize the images of the arterial lumen wall interface. When the tracking gate was placed on the intima, the artery diameter was automatically tracked and the waveform of diameter changes over the cardiac cycle was showed in real time using the FMD mode of the e-TRACKING system. This allowed the ultrasound images to be optimized at the start of the scan and the transducer position to be adjusted immediately for optimal tracking performance throughout the scan. The software could accommodate angulations of the artery from −20 to +20° relative to the perpendicular. Pulsed Doppler flow was assessed at baseline and during peak hyperemic flow, which was confirmed to occur within 15 s after cuff deflation. The Doppler flow signals were captured with customized equipment. Blood flow velocity was calculated from the color Doppler data and was showed as a waveform in real time. The baseline longitudinal image of the artery was acquired for 30 s and then the blood pressure cuff was inflated to 50 mm Hg above systolic pressure for 5 min. The longitudinal image of the artery was recorded continuously until 5 min after cuff deflation. Pulsed Doppler velocity signals were obtained for 20 s at baseline and for 10 s immediately after cuff deflation. Changes in brachial artery diameter were immediately expressed as percent change relative to the vessel diameter before cuff inflation. FMD was automatically calculated as the percent change in peak vessel diameter from the baseline value. %FMD (peak diameter−baseline diameter/baseline diameter) was used for analysis. Blood flow volume was calculated by multiplying the Doppler flow velocity (corrected for the angle) by heart rate and vessel cross-sectional area ($-r^2$). Reactive hyperemia was calculated as the maximum percentage increase in flow after cuff deflation compared with baseline flow. After a 10-min period to allow baseline conditions of the brachial artery to be reestablished, another baseline scan was performed. The response to nitroglycerine (NTG) was used for assessment of endothelium-independent vasodilation. After acquiring baseline resting images for 30 s, a sublingual tablet (NTG 75 μg) was given, and images of the artery were recorded continuously for 5 min. The response of the brachial artery diameter to NTG was immediately expressed as percent change relative to vessel diameter. NTG-induced vasodilation was automatically calculated as the percent change in peak vessel diameter from the baseline value. %NTG (peak diameter−baseline diameter/baseline diameter) was used for analysis. The intra-observer coefficient of variation for the baseline diameter was 3.5% in the supine position and was 2.7% in the seated position. The respective inter-observer coefficients were 2.6 and 1.9%.

Baseline fasting serum concentrations of total cholesterol, high-density lipoprotein cholesterol, low-density lipoprotein cholesterol, triglycerides, glucose, insulin, electrolytes, high-sensitivity CRP and 8-hydroxy-2′-deoxyguanosine (8-OHdG) were obtained after a 30-min rest period before the study.

### Measurement of ROCK activity

ROCK activity was assayed in peripheral blood leukocytes as the amount of phospho-Thr853 in the MBS of myosin light-chain phosphatase. Blood was collected at room temperature in heparinized tubes (20 U ml$^{-1}$) with 10 mmol l$^{-1}$ fasudil (Asahi Chemical Industry, Tokyo, Japan ). Fasudil was added to inhibit ROCK activity and hence further formation of phospho-Thr853 MBS *ex vivo*. After adding an equal volume of 2% dextran, the sample was kept at room temperature for 30 min. The supernatant was spun at 1450 r.p.m. for 10 min. Red blood cells in the resulting cell pellet were lysed with the addition of water and spun at 1450 r.p.m. for 10 min after the addition of Hank's balanced salt solution (Hyclone, Logan, UT, USA). The resulting leukocyte pellet was resuspended in medium 199 (Sigma Chemical) and counted using a hematocytometer. Cells were fixed in 10% trichloroacetic acid and 10 mmol l$^{-1}$ dichlorodiphenyltrichloroethane. After centrifugation, the cell pellets were stored at −80 °C for western blot analysis. Cells pellets were dissolved in 10 μl of 1 mol l$^{-1}$ Tris base and then mixed with 100 μl of extraction buffer (8 mol l$^{-1}$ urea, 2% sodium dodecyl sulfate, 5% sucrose and 5% 2-mercaptoethanol). Equal amounts of cell extracts were subjected to 7.5% sodium dodecyl sulfate-polyacrylamide gel electrophoresis and transferred to nitrocellulose membranes. NIH 3T3 cell lysates were used as a positive control and to standardize the results of western blot analyses from several membranes. After serum starvation for 20 h, confluent cells were stimulated with 10 μmol l$^{-1}$ lysophosphatidic acid for 10 min and then subsequently fixed and harvested in 10% trichloroacetic acid and 10 mmol l$^{-1}$ dichlorodiphenyltrichloroethane. After centrifugation at 1450 r.p.m. for 10 min at 4 °C, precipitates were dissolved in 10 μl of 1 mol l$^{-1}$ Tris base and mixed with 100 μl of extraction buffer. An equal volume of positive control cell lysate was used for each gel. Membranes were incubated with rabbit anti-phospho-specific Thr853–MBS polyclonal antibody (Biosource Invitrogen, Carlsbad, CA, USA) or rabbit anti-MBS polyclonal antibody (Covance Laboratories, Evansville, IN, USA), anti-ROCK2 monoclonal antibody, anti-ROCK1 monoclonal antibody (BD Biosciences, San Jose, CA, USA) or antiactin monoclonal antibody (Sigma). Bands were visualized using the enhanced chemiluminescence system (Amersham-Pharmacia, Buckinghamshire, UK). Images were captured using Adobe Photoshop, and the band intensities were quantified using National Institutes of Health Image 1.61. ROCK activity was expressed as the ratio of phospho-Thr853–MBS in each sample to phospho-Thr853–MBS in each positive control divided by MBS in each sample per MBS in each positive control.

### Analytical methods

Samples of venous blood were placed in tubes containing sodium EDTA (1 mg ml$^{-1}$) and in polystyrene tubes. The EDTA-containing tubes were chilled promptly in an ice bath. Plasma was immediately separated by centrifugation at 3100 *g* for 10 min at 4 °C, and serum was separated by centrifugation at 1000 *g* for 10 min at room temperature. Samples were stored at −80 °C until the time of assay. Serum concentrations of total cholesterol, triglycerides, high-density lipoprotein cholesterol, low-density lipoprotein cholesterol, glucose and electrolytes were determined by routine chemical methods. Serum concentration of high-sensitivity CRP was measured by a high sensitive nephelometry assay using a CRP kit (Dade Behring, Deerfield, IL, USA). Serum concentration of 8-OHdG was also assayed by ELISA using 8-OHdG kits (Nihon Yushi, Fukuroi, Japan).

### Statistical analysis

Results are presented as mean ± s.d. Unpaired Student's *t*-test was used for comparison of mean values of parametric continuous variables between smoker and control groups. Because of asymmetric distribution, values for ROCK activity and the protein expression of MBS, ROCK1 and ROCK2 were analyzed using nonparametric methods. For nonparametric analysis, we used Mann–Whitney *U*-test to evaluate the difference of levels between groups. All reported *P*-values were two sided, and a *P*-value of $<0.05$ was considered statistically significant. Multivariate analysis was performed with the Statistical Analysis System program package (SAS Institute, Cary, NC, USA). The data were analyzed using the software package StatView V (SAS Institute) and Super ANOVA (Abacus Concepts, Berkley, CA, USA).

## RESULTS

### Clinical characteristics

Baseline clinical characteristics of the 14 smokers and 15 non-smokers are summarized in the Table 1. Serum concentration of 8-OHdG was significantly higher in smokers than in non-smokers. There was no significant difference in other parameters between the smokers and non-smokers.

### ROCK activity

ROCK activity in peripheral blood leukocytes was significantly higher in smokers than in non-smokers (0.78 ± 0.27 *vs.* 0.54 ± 018, *P*=0.012; Figure 1b). Protein expression of MBS, ROCK1 and ROCK2 were similar for the smokers and non-smokers (1.91 ± 0.87 *vs.* 2.04 ± 1.60, 1.54 ± 0.85 *vs.* 1.95 ± 1.12, and 1.45 ± 0.56 *vs.* 1.29 ± 0.14, respectively, Figures 1c and d).

Table 1 Clinical characteristics in non-smokers and smokers

| *Variables* | *Non-smoker (n=15)* | *Smoker (n=14)* |
|---|---|---|
| Age (years) | 34.8 ± 6.5 | 35.8 ± 3.8 |
| Body mass index (kg cm$^{-2}$) | 22.3 ± 1.7 | 23.7 ± 2.8 |
| Systolic blood pressure (mm Hg) | 120.1 ± 14.4 | 117.6 ± 11.9 |
| Diastolic blood pressure (mm Hg) | 65.7 ± 9.4 | 67.5 ± 10.5 |
| Heart rate (beats min$^{-1}$) | 65.8 ± 9.6 | 78.3 ± 7.6 |
| Total cholesterol (mg per 100 ml) | 184.1 ± 32.7 | 206.4 ± 31.1 |
| Triglycerides (mg per 100 ml) | 126.9 ± 96.6 | 144.4 ± 66.2 |
| Low-density lipoprotein cholesterol (mg per 100 ml) | 112.4 ± 30.4 | 113 ± 30.4 |
| High-density lipoprotein cholesterol (mg per 100 ml) | 57.9 ± 13.7 | 61.8 ± 22.2 |
| Fasting serum glucose (mg per 100 ml) | 98.9 ± 14.9 | 108.6 ± 10.3 |
| Serum creatinine (mg per 100 ml) | 0.80 ± 0.09 | 0.84 ± 0.06 |
| High-sensitivity C-reactive protein (mg per 100 ml) | 0.05 ± 0.08 | 0.06 ± 0.05 |
| 8-hydroxy-2′-deoxyguanosine (ng ml$^{-1}$) | 0.22 ± 0.03 | 0.28 ± 0.04* |

All results are presented as mean ± s.d.
*$P<0.05$ *vs.* non-smoker.

### Relationship between ROCK activity and parameters

Using univariate linear regression analysis, only systolic blood pressure significantly correlated with ROCK activity ($r$=0.42, $P$=0.039; Table 2 and Figure 2). Multivariate analysis was performed to explain variability (systolic blood pressure and smoking status being associated with ROCK activity) of ROCK activity. Smoking status was an independent predictor of ROCK activity (Table 3).

### Vascular function

FMD was significantly lower in smokers than in non-smokers (4.7 ± 3.1 *vs.* 9.0 ± 3.8%, $P$=0.005; Figure 3a). NTG-induced vasodilation was similar in smokers and non-smokers (16.5 ± 5.8 *vs.* 13.7 ± 5.1%; Figure 3b). Baseline arterial diameter and peak hyperemic blood flow were similar in the two groups (4.3 ± 0.5 *vs.* 4.0 ± 0.4 mm and 306 ± 149 *vs.* 362 ± 167%, respectively).

### Relationship between ROCK activity and FMD

There was a significant correlation between ROCK activity and FMD ($r$=−0.42; $P$=0.035; Figure 4), whereas ROCK activity did not correlate with NTG-induced vasodilation. Using univariate linear regression analysis, no variable other than ROCK activity significantly correlated with FMD (Table 4). There was no significant relationship between NTG-induced vasodilation and parameters.

## DISCUSSION

In this present study we showed that ROCK activity in peripheral blood leukocytes was higher in young male smokers than in non-smokers and was inversely correlated with FMD. Multiple regression analysis revealed that smoking status was an independent predictor of ROCK activity.

We selected young men to avoid the possibility of alteration in ROCK activity and endothelial function caused by factors other than smoking, such as hypertension, heart failure, atherosclerosis, hypercholesterolemia, diabetes mellitus, aging and menstrual cycle.

We have recently reported that intra-arterial infusion of fasudil, which is a broad ROCK inhibitor, increases forearm blood flow in smokers but not in non-smokers, suggesting that ROCK activity may be higher in smokers than in non-smokers.[22] In this study, we confirmed that ROCK activity was increased in smokers using a noninvasive method for measurement of ROCK activity in peripheral blood leukocytes. It is well known that peripheral blood leukocytes *per se* have an important role in the cause, maintenance and development of atherosclerosis. Therefore, our findings suggest that the enhancement of ROCK activity by cigarette smoking may cause leukocyte activation and enhanced leukocyte infiltration into the vascular wall, leading to progression of atherosclerosis. Furthermore, leukocyte ROCK activity has been shown to correlate with endothelial dysfunction.[11] It is clinically important to estimate the degree of ROCK activity. A noninvasive method for measuring leukocyte ROCK activity would also be useful for assessing ROCK activity. Leukocyte ROCK activity may become a novel biomarker of endothelial function and atherosclerosis.

Inflammation has a critical role in the development and complications of atherosclerosis.[13,23] Previous studies have shown that cigarette smoking causes inflammation and increases the numbers of circulating leukocytes and circulating inflammatory markers such as CRP, interleukin-6 and soluble intercellular adhesion molecule type 1.[6]

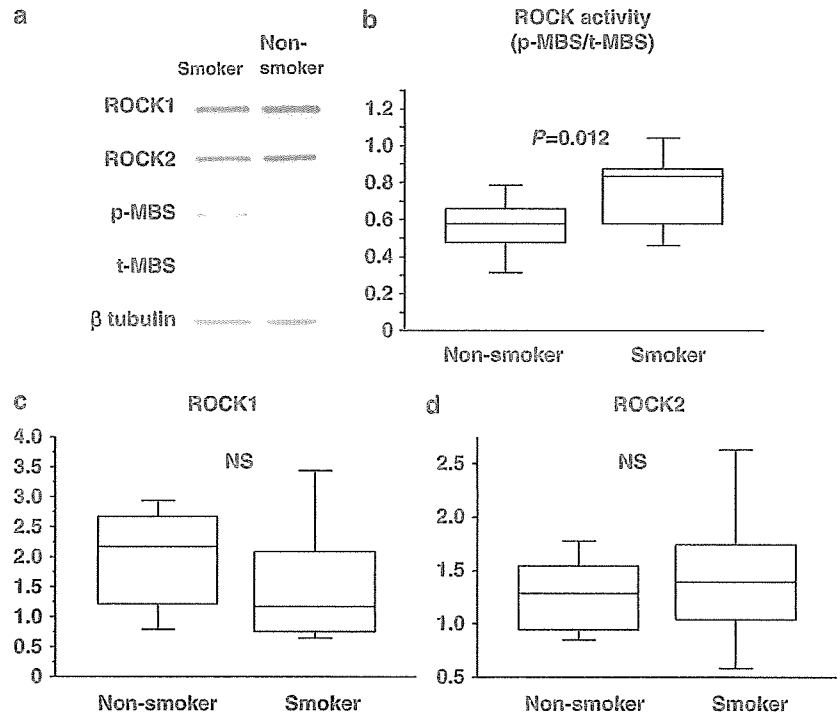


Figure 1 Rho-associated kinase (ROCK) activity in smokers and non-smokers. (a) Western blot analysis for ROCK1, ROCK2, phospho-myosin-binding subunit (p-MBS), total-myosin-binding subunit (t-MBS) and β-tubulin. (b) ROCK activity (p-MBS/t-MBS) in smokers and non-smokers. (c) ROCK1 expression in smokers and non-smokers. (d) ROCK2 expression in smokers and non-smokers.

**Table 2 Simple regression analysis between ROCK activity and variables**

| *Variables* | *Coefficient* | P-*value* |
|---|---|---|
| Age (years) | 0.04 | 0.86 |
| Body mass index (kg cm$^{-2}$) | 0.32 | 0.11 |
| Systolic blood pressure (mm Hg) | 0.42 | 0.04 |
| Diastolic blood pressure (mm Hg) | 0.08 | 0.94 |
| Heart rate (beats min$^{-1}$) | 0.06 | 0.80 |
| Total cholesterol (mg per 100 ml) | 0.35 | 0.10 |
| Triglycerides (mg per 100 ml) | 0.19 | 0.39 |
| Low-density lipoprotein cholesterol (mg per 100 ml) | 0.28 | 0.18 |
| High-density lipoprotein cholesterol (mg per 100 ml) | 0.03 | 0.80 |
| Fasting serum glucose (mg per 100 ml) | 0.24 | 0.23 |
| Serum creatinine (mg per 100 ml) | 0.11 | 0.62 |
| High-sensitivity C-reactive protein (mg per 100 ml) | 0.10 | 0.64 |
| 8-hydroxy-2′-deoxyguanosine (ng ml$^{-1}$) | 0.36 | 0.20 |

Abbreviation: ROCK, Rho-associated kinase.

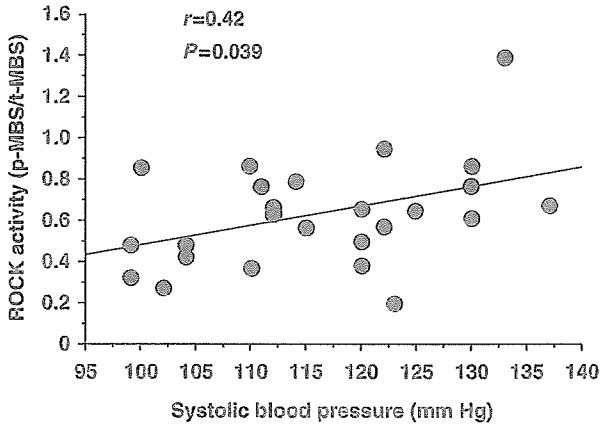


Figure 2 Relationship between Rho-associated kinase (ROCK) activity and systolic blood pressure.

Activation of circulating leukocytes leading to the recruitment and infiltration of inflammatory cells into vessel walls has an important role in the pathogenesis of atherosclerosis.[4,24] ROCKs regulate inflammatory cell accumulation in the vessel wall and contribute to the development of vascular inflammation and remodeling.[13,25] Although the mechanism by which smoking enhances ROCK activity in leukocytes remains unclear, smoking may increase leukocytes chemotaxis and recruitment to the vessel wall through activation of ROCKs. Indeed, deletion of ROCK1 leads to impaired leukocyte chemotaxis and migration.[25,26] In this study, there was no significant difference in high-sensitivity CRP between the smokers and non-smokers. In addition, there was no significant relationship between the number of cigarettes (pack-year) and CRP levels.

Several investigators have shown an interaction between the RhoA/ROCk pathway and reactive oxygen species.[27] Indeed, reactive oxygen species induced by hyperglycemia enhances ROCK activity, leading to atherothrombogenesis through an increase in expression of plasminogen activator inhibitor-1 in vascular endothelial cells.[28] It is well known that cigarette smoking decreases NO bioavailability through the production of reactive oxygen species. Several investigators, including us, have shown that there is a possible association of ROCK activity with oxidative stress and that smoking enhances the

Table 3 Multiple regression analysis for ROCK activity

| *Variables* | *Coefficient* | *s.e.* | *95% CI* | P-*value* |
|---|---|---|---|---|
| Intercept | −0.34 | 0.45 | −1.27–0.59 | 0.46 |
| Systolic blood pressure | 0.01 | 0.003 | −0.001–0.026 | 0.06 |
| Smoking | 0.22 | 0.08 | 0.05–0.38 | 0.01 |

Abbreviations: CI, confidence interval; ROCK, Rho-associated kinase.

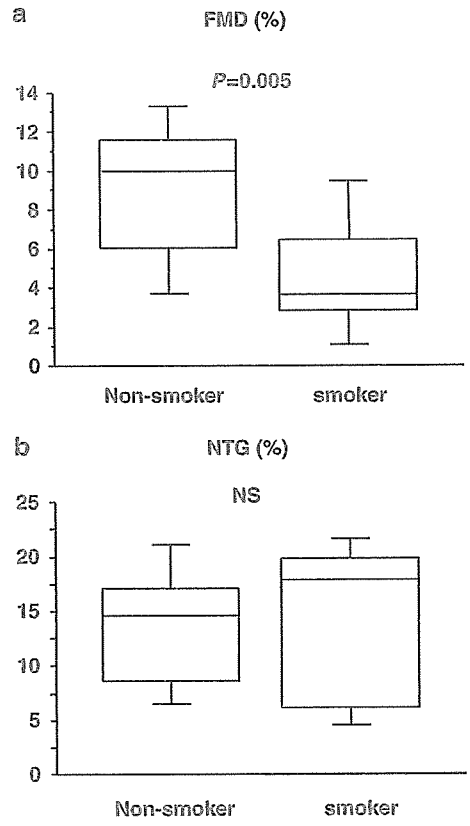


Figure 3 Vascular function in smokers and non-smokers. (a) Flow-mediated vasodilation (FMD) in the smokers and non-smokers. (b) Nitroglycerine (NTG)-induced vasodilation in smokers and non-smokers.

activation of ROCKs in vascular smooth muscle cells *in vivo* and *in vitro*.[22,27,29] Excess oxidative stress may have a role in the smoking-induced activation of ROCKs in leukocytes. Increase in ROCK activity in vascular endothelial cells directly alters FMD through the inactivation of eNOS. It is well known that activation of ROCK induces various substrates and transcriptional factors, leading to actin cytoskeleton organization, smooth muscle contraction, vascular inflammation, apoptosis and gene expression differentiation. Under the condition of excessive reactive oxygen species by smoking, oxidative stress and activated ROCK-induced impairment of various cellular functions may cause a vicious circle. Thus, activated ROCK in vascular smooth muscle cells and in leukocytes may also contribute to impaired FMD through increase in oxidative stress. In this study, serum concentration of 8-OHdG was significantly higher in smokers than in non-smokers. However, univariate and multiple regression analyses revealed that 8-OHdG was not an independent predictor of ROCK activity.

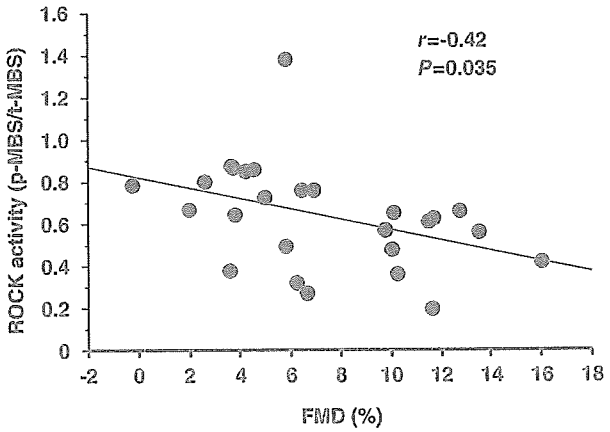


Figure 4 Relationship between Rho-associated kinase (ROCK) activity and flow-mediated vasodilation (FMD).

Table 4 Simple regression analysis between FMD activity and variables

| *Variables* | *Coefficient* | P-*value* |
|---|---|---|
| Age (years) | 0.12 | 0.56 |
| Body mass index (kg cm$^{-2}$) | 0.17 | 0.44 |
| Systolic blood pressure (mm Hg) | 0.22 | 0.30 |
| Diastolic blood pressure (mm Hg) | 0.17 | 0.36 |
| Heart rate (beats min$^{-1}$) | 0.32 | 0.16 |
| Total cholesterol (mg per 100 ml) | 0.39 | 0.09 |
| Triglycerides (mg per 100 ml) | 0.23 | 0.32 |
| Low-density lipoprotein cholesterol (mg per 100 ml) | 0.23 | 0.33 |
| High-density lipoprotein cholesterol (mg per 100 ml) | 0.36 | 0.12 |
| Fasting serum glucose (mg per 100 ml) | 0.16 | 0.47 |
| Serum creatinine (mg per 100 ml) | 0.17 | 0.48 |
| High-sensitivity C-reactive protein (mg per 100 ml) | 0.18 | 0.45 |
| 8-hydroxy-2′-deoxyguanosine (ng ml$^{-1}$) | 0.16 | 0.63 |
| Rho-associated kinase activity | 0.42 | 0.03 |

Abbreviation: FMD, flow-mediated vasodilation.

Interestingly, ROCK activity significantly correlated with systolic blood pressure even in the young male subjects with normal blood pressure. This finding is supported by results of previous studies showing that the ROCKs are involved in the pathogenesis of hypertension through, at least in part, causing vascular smooth muscle cell contraction.[9,16,30] There is a possibility that ROCK activity regulates blood pressure from the normal range to high levels. However, multivariate regression analysis revealed that smoking but not blood pressures independently correlated with ROCK activity.

FMD, as an index of endothelium-dependent vasodilation, was impaired even in young smokers compared with non-smokers. These findings are consistent with results of previous studies showing that smoking is associated with endothelial dysfunction.[5,22] One of the important findings in this study is a significant relationship between ROCK activity in peripheral leukocytes and FMD in smokers. As Sauzeau *et al.*[30] have shown in vascular smooth muscle cells, NO may also inhibit RhoA translocation from the cytosol to membrane in leukocytes. In addition, previous studies have shown that activation of the RhoA/ROCK pathway impairs NO bioavailability through the inhibition of eNOS mRNA stability, eNOS posphorylation at Ser 1177, Akt/phosphoinositide 3-kinase pathway and enhancement of eNOS

phosphorylation at Thr495.[20,22] Taken together, the results indicate that ROCK activity in leukocytes may reflect ROCK activity in vascular endothelial cells and endothelial function, suggesting an interaction between ROCK activity and endogenous NO.

### Limitation

We hypothesized that smoking causes inflammation, leading to enhancement of ROCK activity. However, serum levels of CRP, which is a marker of systemic inflammation, were similar in smokers and non-smokers. The discrepancy in the effect of smoking on inflammation between the present study and previous studies may be due to the limited number of subjects in each group, differences in age (our subjects being younger), the magnitude of smoking (our subjects having a smaller number of pack-years) and body mass index BMI (our subjects having smaller body mass index).[9,21] In addition, the levels of CRP in smokers and non-smokers in this study were $<0.2$ mg per 100 ml. The levels of CRP in this study were lower than those in previous studies showing a relationship between smoking and CRP levels.[9,21] In those previous studies, the levels of CRP in smokers were $>0.2$ mg per 100 ml. However, we cannot exclude the possibility that inflammation caused by smoking contributes to the enhancement of ROCK activity. Further studies are required with other inflammatory biomarkers to determine whether there is any relationship between inflammation and ROCK activity.

In conclusion, measurement of ROCK activity in peripheral leukocytes is minimally invasive and does not require pharmacologic intervention (for example, intra-arterial or intravenous infusion of ROCK inhibitors) and may be useful as a novel predictor of atherosclerotic disease in a clinical setting. It remains to be determined whether ROCK activity is a predictor of cardiovascular outcome.

## ACKNOWLEDGEMENTS

We thank Megumi Wakisaka, Keiko Umeda and Satoko Michiyama for their excellent secretarial assistance. This study was supported in part by a Grant-in-Aid for Scientific Research from the Ministry of Education, Science and Culture of Japan (1559075100 and 1859081500), and the National Institutes of Health (HL052233 and HL08187).

## CONFLICT OF INTEREST

Dr James K Liao is a consultant for Asahi-Kasei Pharmaceutical.

1 Howard G, Wagenknecht LE, Burke GL, Diez-Roux A, Evans GW, McGovern P, Nieto FJ, Tell GS. Cigarette smoking and progression of atherosclerosis: the Atherosclerosis Risk in Communities (ARIC) study. *JAMA* 1998; **279**: 119–124.
2 Tell GS, Polak JF, Ward BJ, Kittner SJ, Savage PJ, Robbins J. Relation of smoking with carotid artery wall thickness and stenosis in older adults. The Cardiovascular Health Study. The Cardiovascular Health Study (CHS) Collaborative Research Group. *Circulation* 1994; **90**: 2905–2908.
3 Barua RS, Ambrose JA, Eales-Reynolds LJ, DeVoe MC, Zervas JG, Saha DC. Dysfunctional endothelial nitric oxide biosynthesis in healthy smokers with impaired endothelium-dependent vasodilatation. *Circulation* 2001; **104**: 1905–1910.
4 Libby P, Ridker PM, Maseri A. Inflammation and atherosclerosis. *Circulation* 2002; **105**: 1135–1143.
5 Celermajer DS, Adams MR, Clarkson P, Robinson J, McCredie R, Donald A, Deanfield JE. Passive smoking and impaired endothelium-dependent arterial dilatation in healthy young adults. *N Engl J Med* 1996; **334**: 150–155.
6 Tracy RP, Psaty BM, Macy E, Bovill EG, Cushman M, Cornell ES, Kuller LH. Lifetime smoking exposure affects the association of C-reactive protein with cardiovascular disease risk factors and subclinical disease in healthy elderly subjects. *Arterioscler Thromb Vasc Biol* 1997; **17**: 2167–2176.
7 Bermudez EA, Rifai N, Buring JE, Manson JE, Ridker PM. Relation between markers of systemic vascular inflammation and smoking in women. *Am J Cardiol* 2002; **89**: 1117–1119.
8 Amano M, Chihara K, Kimura K, Fukata Y, Nakamura N, Matsuura Y, Kaibuchi K. Formation of actin stress fibers and focal adhesions enhanced by Rho-kinase. *Science* 1997; **275**: 1308–1311.
9 Uehata M, Ishizaki T, Satoh H, Ono T, Kawahara T, Morishita T, Tamakawa H, Yamagami K, Inui J, Maekawa M, Narumiya S. Calcium sensitization of smooth muscle mediated by a Rho-associated protein kinase in hypertension. *Nature* 1997; **389**: 990–994.
10 Hall A. Rho GTPases and the actin cytoskeleton. *Science* 1998; **279**: 509–514.
11 Nohria A, Grunert ME, Rikitake Y, Noma K, Prsic A, Ganz P, Liao JK, Creager MA. Rho kinase inhibition improves endothelial function in human subjects with coronary artery disease. *Circ Res* 2006; **99**: 1426–1432.
12 Kimura K, Fukata Y, Matsuoka Y, Bennett V, Matsuura Y, Okawa K, Iwamatsu A, Kaibuchi K. Regulation of the association of adducin with actin filaments by Rho-associated kinase (Rho-kinase) and myosin phosphatase. *J Biol Chem* 1998; **273**: 5542–5548.
13 Mallat Z, Gojova A, Sauzeau V, Brun V, Silvestre JS, Esposito B, Merval R, Groux H, Loirand G, Tedgui A. Rho-associated protein kinase contributes to early atherosclerotic lesion formation in mice. *Circ Res* 2003; **93**: 884–888.
14 Seasholtz TM, Wessel J, Rao F, Rana BK, Khandrika S, Kennedy BP, Lillie EO, Ziegler MG, Smith DW, Schork NJ, Brown JH, O'Connor DT. Rho kinase polymorphism influences blood pressure and systemic vascular resistance in human twins: role of heredity. *Hypertension* 2006; **47**: 937–947.
15 Rikitake Y, Oyama N, Wang CY, Noma K, Satoh M, Kim HH, Liao JK. Decreased perivascular fibrosis but not cardiac hypertrophy in ROCK1+/– haploinsufficient mice. *Circulation* 2005; **112**: 2959–2965.
16 Masumoto A, Hirooka Y, Shimokawa H, Hironaga K, Setoguchi S, Takeshita A. Possible involvement of Rho-kinase in the pathogenesis of hypertension in humans. *Hypertension* 2001; **38**: 1307–1310.
17 Masumoto A, Mohri M, Shimokawa H, Urakami L, Usui M, Takeshita A. Suppression of coronary artery spasm by the Rho-kinase inhibitor fasudil in patients with vasospastic angina. *Circulation* 2002; **105**: 1545–1547.
18 Vane JR, Anggard EE, Botting RM. Regulatory functions of the vascular endothelium. *N Engl J Med* 1990; **323**: 27–36.
19 Vanhoutte PM. Endothelium and control of vascular function. State of the art lecture. *Hypertension* 1989; **13**(6 Pt 2): 658–667.
20 Wolfrum S, Dendorfer A, Rikitake Y, Stalker TJ, Gong Y, Scalia R, Dominiak P, Liao JK. Inhibition of Rho-kinase leads to rapid activation of phosphatidylinositol 3-kinase/protein kinase Akt and cardiovascular protection. *Arterioscler Thromb Vasc Biol* 2004; **24**: 1842–1847.
21 Liu PY, Chen JH, Lin LJ, Liao JK. Increased Rho kinase activity in a Taiwanese population with metabolic syndrome. *J Am Coll Cardiol* 2007; **49**: 1619–1624.
22 Noma K, Higashi Y, Jitsuiki D, Hara K, Kimura M, Nakagawa K, Goto C, Oshima T, Yoshizumi M, Chayama K. Smoking activates rho-kinase in smooth muscle cells of forearm vasculature in humans. *Hypertension* 2003; **41**: 1102–1105.
23 Lusis AJ. Atherosclerosis. *Nature* 2000; **407**: 233–241.
24 Serrano Jr CV, Ramires JA, Venturinelli M, Arie S, D'Amico E, Zweier JL, Pileggi F, da Luz PL. Coronary angioplasty results in leukocyte and platelet activation with adhesion molecule expression. Evidence of inflammatory responses in coronary angioplasty. *J Am Coll Cardiol* 1997; **29**: 1276–1283.
25 Noma K, Rikitake Y, Oyama N, Yan G, Alcaide P, Liu PY, Wang H, Ahl D, Sawada N, Okamoto R, Hiroi Y, Shimizu K, Luscinskas FW, Sun J, Liao JK. ROCK1 mediates leukocyte recruitment and neointima formation following vascular injury. *J Clin Invest* 2008.
26 Wang HW, Liu PY, Oyama N, Rikitake Y, Kitamoto S, Gitlin J, Liao JK, Boisvert WA. Deficiency of ROCK1 in bone marrow-derived cells protects against atherosclerosis in LDLR–/– mice. *FASEB J* 2008; **22**: 3561–3570.
27 Bailey SR, Mitra S, Flavahan S, Flavahan NA. Reactive oxygen species from smooth muscle mitochondria initiate cold-induced constriction of cutaneous arteries. *Am J Physiol Heart Circ Physiol* 2005; **289**: H243–H250.
28 Rikitake Y, Liao JK. Rho-kinase mediates hyperglycemia-induced plasminogen activator inhibitor-1 expression in vascular endothelial cells. *Circulation* 2005; **111**: 3261–3268.
29 Noma K, Goto C, Nishioka K, Jitsuiki D, Umemura T, Ueda K, Kimura M, Nakagawa K, Oshima T, Chayama K, Yoshizumi M, Liao JK, Higashi Y. Roles of rho-associated kinase and oxidative stress in the pathogenesis of aortic stiffness. *J Am Coll Cardiol* 2007; **49**: 698–705.
30 Sauzeau V, Le Jeune H, Cario-Toumaniantz C, Smolenski A, Lohmann SM, Bertoglio J, Chardin P, Pacaud P, Loirand G. Cyclic GMP-dependent protein kinase signaling pathway inhibits RhoA-induced Ca2+ sensitization of contraction in vascular smooth muscle. *J Biol Chem* 2000; **275**: 21722–21729.

JACC Img, in press.

# Association Between Visceral Adipose Tissue Area and the Vulnerable Characteristics of Noncalcified Coronary Plaques Assessed by 64-Slice Computed Tomographic Angiography

Norihiko Ohashi, MD,* Hideya Yamamoto, MD, PhD, FACC,* Jun Horiguchi, MD, PhD,† Toshiro Kitagawa, MD, PhD,* Eiji Kunita, MD,* Hiroto Utsunomiya, MD,* Toshiharu Oka, MD,* Yasuki Kihara, MD, PhD, FACC*

*Department of Cardiovascular Medicine, Graduate School of Biomedical Sciences, Hiroshima University, Hiroshima, Japan; †Department of Clinical Radiology, Hiroshima University Hospital, Hiroshima, Japan.

**Address for correspondence:** Hideya Yamamoto, MD, Department of Cardiovascular Medicine, Graduate School of Biomedical Sciences, Hiroshima University, 1-2-3 Kasumi Minami-ku, Hiroshima 734-8551, Japan.
Tel: +81-82-257-5540
Fax: +81-82-257-1569
E-mail: hideyayama@hiroshima-u.ac.jp

**Brief title**: Visceral Adiposity and Vulnerable Plaques on CTA
**Total words count**: 4702 words
**Conflict of interest**: none

## Abstract

**Objectives**

We sought to investigate the association of visceral adipose tissue (VAT) with the presence, extent, and characteristics of noncalcified coronary plaques (NCPs) using 64-slice computed tomographic angiography (CTA).

**Background**

Although visceral adiposity is associated with adverse cardiovascular events, its association with NCP burden and vulnerability is not well known.

**Methods**

The study population consisted of 427 Japanese patients (age, 67 ± 11 years; 63% men) with proven or suspected coronary artery disease undergoing 64-slice CTA. We evaluated the vulnerable characteristics of NCPs with positive remodeling (remodeling index > 1.05), low CT density (≤ 38 HU), and the presence of adjacent spotty calcium. Plain abdominal scans were also performed to measure the VAT area.

**Results**

A total of 260 (61%) patients had identifiable NCPs. Multivariate analyses revealed that increased VAT area (per 1 standard deviation, 58 $cm^2$) was significantly associated with both the presence [odds ratio (OR) 1.79; 95% confidence interval (CI) 1.22 to 2.77] and extent (β-estimate 0.34, p = 0.001) of NCP. Increased VAT area was also independently associated with the presence of NCP with positive remodeling (OR 1.69; 95% CI 1.16 to 2.51), low CT density (OR 1.57; 95% CI 1.08 to 2.32), and adjacent spotty calcium (OR 1.53; 95% CI 1.03 to 2.31).

**Conclusions**

Increased VAT is significantly associated with NCP burden and vulnerable characteristics identified by 64-slice CTA. Our findings may explain the excessive cardiovascular risk in patients with visceral adiposity, and support the potential role of CTA to improve risk stratification in such patients.

**Keywords:** visceral adipose tissue, noncalcified coronary plaque, plaque vulnerability, 64-slice computed tomographic angiography

**Abbreviations and Acronyms**

ACS = acute coronary syndrome
BMI = body mass index
CAC = coronary artery calcium
CAD = coronary artery disease
CT = computed tomography
CTA = computed tomographic angiography
IVUS = intravascular ultrasound
NCP = noncalcified coronary plaque
PR = positive remodeling
VAT = visceral adipose tissue

It is well accepted that obesity is a risk factor for coronary artery disease (CAD) (1). Specifically, visceral adipose tissue (VAT) accumulation has been focused as a better predictor of metabolic abnormalities and atherosclerosis than total body fat (2, 3). Recent epidemiological studies have suggested that visceral adiposity, as evaluated by the waist-to-hip ratio (4) or computed tomography (CT) scanning (5), is more closely related to cardiovascular events than body mass index (BMI), as a crude marker of total adiposity.

We previously reported that VAT area is associated with the presence and extent of coronary artery calcium (CAC), independently of BMI, using multi-detector CT (6). However, CAC represents only a limited portion of the overall atherosclerotic plaque

burden. The residual plaque burden is composed of noncalcified coronary plaque (NCP), which might be associated with acute coronary syndrome (ACS) (7-9). Previous intravascular ultrasound (IVUS) (7) and pathologic (8) studies have underscored the critical importance of positive vessel remodeling and large lipid cores as the characteristics of ruptured plaques which are considered to be the major substrate for ACS. In addition, spotty calcifications embedded in atherosclerotic lesions have been shown to contribute to plaque instability (10).

The recently introduced multi-detector computed tomographic angiography (CTA) is a robust and reliable noninvasive imaging modality that permits visualization of the coronary artery wall and was shown to detect calcified and noncalcified plaques with good correlation to IVUS (11). Moreover, we previously reported that 64-slice CTA allows the characterization of NCPs such as composition (e.g, predominantly fibrous vs. lipid-rich plaque), vascular remodeling, and adjacent calcium morphology, showing good agreement with IVUS (12). We further documented that low CT density, positive remodeling (PR), and the presence of adjacent spotty calcium are "vulnerable" features of NCPs, which characterize ACS culprit lesions (13).

To our knowledge, very few studies have examined the association between VAT, as an entity, with NCP, particularly regarding its composition and morphology. Assessing the associations between VAT area and NCP burden or vulnerable characteristics seems to be important from preventive perspectives. Therefore, in the present study, we used 64-slice CTA to quantitatively and qualitatively assess coronary artery plaques to test whether the amount of VAT is associated with the presence, extent, and vulnerable characteristics of NCPs.

## Methods

### Study patients

Between November 2006 and December 2008, we recruited 565 consecutive Japanese patients with proven or suspected CAD, who underwent 64-slice CTA for the follow-up or diagnosis of CAD in our institution. For the present study, we excluded 138 subjects with a history of percutaneous coronary intervention (n = 63) or coronary artery bypass grafting (n = 62), subjects with poor image quality due to motion artifacts or inadequate contrast concentration (n = 6), and subjects with missing information on one or more traditional CAD risk factors (n = 7). As a result, a total of 427 patients (267 men and 160 women, 67 ± 11 years) were finally enrolled and included in this study. In all patients, plain cardiac and abdominal scans were performed to measure the CAC score and the VAT area. The study was approved by the hospital's ethical committee, and written informed consent was obtained from all patients.

### Risk factor assessment

All patients provided details of their demographics, medical history, and medications at the clinical consultation. Patients were considered current smokers if they had smoked at least one cigarette per day within the previous year. Hypertension was defined as systolic blood pressure ≥ 140 mmHg, diastolic blood pressure ≥ 90 mmHg, or on antihypertensive therapy. Diabetes mellitus was defined by self-report, a fasting plasma glucose level ≥ 126 mg/dl, or current use of hypoglycemic agents. Hypercholesterolemia was characterized by a fasting serum low-density lipoprotein cholesterol level ≥ 140 mg/dl on direct measurement (14) or current use of lipid-lowering agents. Height (m) and body weight (kg) were used to calculate the BMI.

**Coronary CT scan protocol and reconstruction**

CT examinations were performed using a 64-slice CT scanner (LightSpeed VCT, GE Healthcare, Waukesha, Wisconsin) with a gantry rotation time of 350 ms. In order to avoid motion artifacts in patients with high heart rates, oral medication with 40 mg metoprolol 60 min before the CT scan was administered to patients with a resting heart rate ≥ 60 beats/min. All patients received 0.3 mg nitroglycerin sublingually just before scanning. A non contrast-enhanced scan with prospective electrocardiographic gating was performed before CTA to measure the CAC score according to the Agatston method (sequential scan with 16 × 2.5 mm collimation; tube current, 140 mA; tube voltage, 120 kV). Following a test bolus examination to determine the start of the contrast-enhanced scan, retrospective electrocardiogram-gated CTA was performed using a helical mode during an inspiratory breath-hold (64 × 0.625 mm collimation; CT pitch factor, 0.18 – 0.24:1; tube current, 600 – 750 mA with electrocardiogram correlated tube current modulation; tube voltage, 120 kV). A body weight-adapted volume (0.6 – 0.7 ml/kg) of contrast material (Iopamidol, 370 mg I/ml, Bayer Healthcare, Berlin, Germany) was injected over the course of 10 seconds, followed by a saline flush of 25 ml. The effective radiation dose was estimated based on the dose-length product and ranged from 15 to 18 mSv (12).

Image reconstruction was retrospectively gated to the electrocardiogram. Depending on the heart rate, either a half-scan (temporal window = 175 ms) or a multi-segment (temporal window < 175 ms) reconstruction algorithm was selected, and the optimal cardiac phase with the fewest motion artifacts was chosen individually. The reconstructed image data were transferred to a remote computer workstation for post-processing (Advantage Workstation Ver.4.2, GE Healthcare) and analyzed using dedicated software (CardIQ™, GE Healthcare).

**Evaluation of NCP characteristics**

All coronary segments > 2 mm in diameter were evaluated by two blinded and independent observers using curved multiplanar reconstructions and cross-sectional images rendered perpendicular to the vessel center line. The definitions of NCP and coronary calcium were as follows (12): NCP, a low-density mass > 1 $mm^2$ in size,

located within the vessel wall and clearly distinguishable from the contrast-enhanced coronary lumen and the surrounding pericardial tissue; coronary calcium, a structure on the vessel wall with a CT density greater than that of the contrast-enhanced coronary lumen, or with a CT density of > 130 HU assigned to the coronary artery wall in a plain image. For NCP and calcium analyses, the optimal image display setting was chosen on an individual basis; in general, the window was between 700 and 1000 HU and the level was between 100 and 200 HU.

We evaluated NCP characteristics on CTA by determining the minimum CT density, vascular remodeling index, and adjacent calcium morphology, as previously described (12). The minimum CT density was determined as the lowest density of at least five regions of interest (area = 1 $mm^2$), which was placed in each lesion in a random order. Based on our comparison of CTA and IVUS data (12), we defined NCP ≤ 38 HU (corresponding to IVUS-identified hypoechoic plaque) as a low-density plaque. We then measured the cross-sectional vessel area ($mm^2$) at each NCP site by manually tracing the outer vessel contour (border to low-signal epicardial fat). Vascular remodeling was assessed using the remodeling index, which was calculated by dividing the cross-sectional lesion vessel area by the proximal reference vessel area. PR was defined as remodeling index > 1.05 (12). Finally, we assessed calcium deposits in or adjacent to each NCP by determining their presence or absence, and their morphology. Spotty calcium was defined as follows: length of calcium burden < $^3/_2$ of the vessel diameter and width < $^2/_3$ of the vessel diameter (15).

**Measurement of VAT area**

In addition to cardiac scans, abdominal scans were performed at the 4 – 5th lumbar levels in spine position, and single 5-mm slices were taken during suspended respiration after normal expiration. The adipose tissue areas and waist circumference in each subject were determined from an image at the level of the umbilicus using dedicated software (Virtual Place, AZE Inc., Tokyo, Japan). Subcutaneous adipose tissue was defined as extraperitoneal fat between the skin and muscles, with attenuation ranging from –150 to –50 HU. Intraperitoneal fat with the same density as the subcutaneous adipose tissue layer was defined as VAT. The adipose tissue areas were determined by automatic planimetry. The waist circumference was determined at the umbilicus level using a mobile caliper.

**Statistical analysis**

Categorical variables are presented as number of patients (percentage), and continuous variables are expressed as means ± standard deviation (SD) or medians (interquartile range). We compared sex-specific clinical and CTA characteristics between patients divided by the median values of VAT area. Differences between patients with high and low VAT area were evaluated using $\chi^2$-test for categorical variables and Student's t test or the Mann-Whitney U test for continuous variables. The

presence of NCP was assessed as a binary outcome and the extent of NCP was defined as a continuous variable indicating the number of detectable NCPs. Stratified analyses were also performed according to the vulnerable NCP characteristics (PR, low CT density, and spotty calcium). Multivariate logistic and linear regression analyses were performed to determine whether the association between VAT area and the presence and extent of NCP was independent of age, sex, traditional risk factors (hypertension, hypercholesterolemia, diabetes mellitus, current smoking, and medications), and other adiposity indices (BMI, subcutaneous adipose tissue, and waist circumference). We further assessed the relationship between VAT area and the presence of vulnerable NCP characteristics using age- and sex-adjusted, and multivariate logistic regression models in a hierarchal fashion. All analyses were done using JMP 5.0.1 statistical software (SAS Institute Inc, Cary, North Carolina). A p-value of $< 0.05$ was considered statistically significant.

# Results

### Patient characteristics

Table 1 lists the clinical characteristics of the study patients according to the median VAT area (men, 126 $cm^2$; women, 91 $cm^2$). Compared with patients with low VAT area, those with high VAT area had a higher BMI, waist circumference, and subcutaneous adipose tissue area, and a higher prevalence of hypertension, hypercholesterolemia, and diabetes mellitus in both sexes. In addition, the triglyceride and hemoglobin A1c levels were higher and that of high-density lipoprotein cholesterol was lower in patients with high VAT in both sexes. With respect to medications, patients with high VAT area had a higher prevalence of using antihypertensive agents in men, and hypoglycemic agents in both sexes.

### CTA plaque characteristics

Of 427 patients, 95 (22%) had no coronary plaques. Of the remaining 332 (78%) patients, although only calcified plaques were observed in 72 (17%) and NCPs were detected in 260 (61%, 189 men). A total of 576 NCPs were visualized (mean 2.2 ± 1.1 per patient) and the NCPs were localized to the left main trunk (n = 57), left anterior descending artery (n = 245), left circumflex artery (n = 103), and the right coronary artery (n = 171). Of 427 patients, 120 patients (28%) had a $\geq$ 50% stenotic lesion in at least 1 coronary vessel. The number of patients with NCPs with PR (remodeling index > 1.05), low CT density ($\leq$ 38 HU), and adjacent spotty calcium deposits was 166 (39%), 159 (37%), and 114 (27%), respectively. Seventy-one patients (17%) had NCP with all three characteristics.

### Comparisons of plaque burden and vulnerable characteristics between patients

**with high and low VAT area**

Figure 1 shows a representative CTA finding in a patient with high VAT area presenting with unstable angina pectoris. Figure 2 shows the prevalence of NCP characteristics in patients with high and low VAT area. Compared with patients with low VAT, those with high VAT were more likely to have NCP in men (82% vs. 60%, $p < 0.0001$) and in women (56% vs. 33%, $p = 0.003$). In analyses stratified for vulnerable NCP characteristics, patients with high VAT had a higher prevalence of NCP with PR (59% vs. 30%, $p < 0.0001$), low CT density (55% vs. 34%, $p = 0.0007$), and adjacent spotty calcium (41% vs. 26%, $p = 0.01$) in men and PR (41% vs. 18%, $p = 0.001$) and low CT density (34% vs. 16%, $p = 0.01$) in women. The frequency of patients with NCP with all three characteristics was higher in men with high VAT (29% vs. 13%, $p = 0.001$). Figure 3 shows the comparison of CAC score and the number of NCPs between patients with high and low VAT. In both sexes, patients with high VAT area were more likely to have high CAC score [138 (18 – 342) vs. 60 (0 – 292), $p = 0.008$ in men, 46 (0 – 246) vs. 0 (0 – 45), $p = 0.0001$ in women] and a greater extent of NCP distribution (mean; $2.0 \pm 1.4$ vs. $1.3 \pm 1.3$, $p = 0.0001$ in men, $1.2 \pm 1.4$ vs. $0.7 \pm 1.2$, $p = 0.007$ in women) than those with low VAT.

**Multivariate associations of VAT area with NCP burden and vulnerable characteristics**

Table 2 shows the association between VAT area and clinical variables with the presence and extent of NCP in all patients. In addition to age and traditional coronary risk factors such as hypertension, hypercholesterolemia, diabetes mellitus, and current smoking, increased VAT area (per 1-SD, 58 $cm^2$) was significantly associated with the presence [odds ratio 1.79; 95% confidence interval 1.22 to 2.77] and extent (β-estimate 0.34, $p = 0.001$) of NCP. Despite positive correlations between other adiposity measurements and VAT (age- and sex-adjusted Pearsons' correlation coefficient vs. VAT: 0.65 for BMI, 0.77 for waist circumference, and 0.53 for subcutaneous adipose tissue; $p < 0.0001$ for all), these adiposity variables had no associations with NCP. The results of age- and sex-adjusted and multivariate analyses of the association between VAT and vulnerable NCP characteristics are depicted in Table 3. Increased VAT area was an independent factor associated with the presence of NCP with PR, low CT density, and adjacent spotty calcium.

## Discussion

In the present study, we showed that the amount of VAT was significantly associated with the presence and extent of NCP, as detected by 64-slice CTA. This association was independent of traditional coronary risk factors. Taken together with our previous reports (6), the present data indicate that visceral adiposity was associated

with a higher likelihood of having CAD and, if present, more diffuse CAD compared with patients without visceral adiposity. Importantly, the study also demonstrated that high VAT area was significantly associated with the presence of NCP with PR, low CT density, and spotty calcium, which may represent vulnerable characteristics, as previously described (9, 12, 13). Thus, our data support the possibility that the accumulation of VAT could contribute not only to the acceleration of atherosclerosis but also to plaque vulnerability.

**Association between VAT area and coronary plaque burden in 64-slice CTA**

We have reported that the accumulation of VAT is an independent predictor of the presence and extent of CAC by multi-detector CT (6). Despite several epidemiological studies, there is a paucity of data regarding the direct association of VAT with the distribution of NCP. While quantification of CAC is considered to provide prognostic information (16), a recent CTA study suggested that the number of NCPs with a calcified component (namely, mixed plaques) was an independent predictor of acute cardiac events (17). In the present study, we found a positive association between VAT accumulation and NCP burden using 64-slice CTA. These findings may have important therapeutic implications that information about the plaque burden determined by CTA may help to identify patients with visceral adiposity at high risk for cardiovascular events and that identification of such patients is essential to initiate aggressive therapeutic strategies, such as lifestyle modification and pharmacological interventions.

The present data suggest that VAT accumulation accelerates atherosclerosis, independently of traditional cardiovascular risk factors such as hypertension, hypercholesterolemia, and diabetes. These observations may contribute to our understanding that the nontraditional risk factors such as hyperinsulinemia and elevated apolipoprotein B and small low-density lipoprotein particles, which are commonly found in patients with visceral adiposity, may increase the risk of CAD beyond that predicted by the presence of traditional risk factors (18). Notably, smoking showed the higher odds ratio for NCP than VAT in a multivariate model, suggesting that it may possibly facilitate the accumulation of VAT. Taking into account the previous report that smoking habits are independently related to VAT (19), smoking may be the potential confounder in the relation between VAT and CAD risk.

BMI was not significantly related to NCP in the present study. We have also shown that BMI and VAT area were only moderately related, indicating that BMI and VAT carry different information. Interestingly, we found that subcutaneous adipose tissue tended to be protective for NCP, which confirms previous results that subcutaneous adiposity has favorable effects on CAD (4).

**Association between VAT area and the vulnerability of NCP**

Several epidemiological studies have suggested that visceral adiposity is linked to the development of ACS (4, 5). However, its association with coronary plaque

vulnerability is unclear. Several prior CTA studies have indicated that NCP is associated, more so than calcified coronary plaque, with the occurrence of ACS (9). Moreover, we previously documented that PR, low CT density, and adjacent spotty calcium represent CTA-detected plaque vulnerability (13). In the present study, using 64-slice CTA, we provide definitive evidence of increased coronary plaque vulnerability in patients with visceral adiposity.

Although there are many pathways by which visceral adiposity is causally linked to atherosclerosis, one possible mechanism proposed recently is that adipocytokines secreted from VAT, including tumor necrosis factor-α, IL-6, free fatty acids, adiponectin, and plasminogen activator-1, may directly influence the vessel wall atherogenic environment by regulating gene expression and function of endothelial, arterial smooth muscle, and macrophage cells (20). For example, insulin resistance, which is promoted by free fatty acids, is thought to increase atherogenesis and atherosclerotic plaque instability by inducing proinflammatory activities in vascular and immune cells (21). Furthermore, increased levels of plasminogen activator-1 can inhibit plasminogen-induced migration of vascular smooth muscle cell proliferation, leading to plaques that are prone to rupture with thin fibrous caps, necrotic cores and rich in macrophages (22).

Taken together, our findings may partially explain the excess risk in visceral adipose patients, suggesting that elevated VAT accumulation is associated with a pro-inflammatory metabolic profile that is predictive of an unstable atherosclerotic plaque. Therefore, stabilization of the atherosclerotic plaque may offer a legitimate therapeutic target to reduce the risk of ACS in patients with visceral adiposity.

### Study limitations

First, although our data support the notion that VAT is an important factor in the pathogenesis of atherosclerosis, causality cannot be established since this is a cross-sectional study. Prospective and larger population studies are needed to elucidate whether the occurrence of CTA-detected vulnerable NCP in combination with increased VAT area might be a useful tool to identify patients at high risk for cardiovascular events. Second, the study population comprised patients with proven or suspected CAD; thus, our results do not apply to patients with a lower probability of CAD. Finally, the current appropriate clinical guidelines do not recommend screening with CTA because of the high radiation exposure, the use of contrast agents, cost effectiveness, and limited evidence (30). However, investigational studies using CTA should be encouraged to better understand the role of detecting the plaque burden and vulnerability in patients with visceral adiposity, which may help improve risk prediction and the prevention of such events.

## Conclusions

We have demonstrated that increased VAT is significantly associated with the